Contribution of Entanglements to the Equilibrium Modulus of 1,2-Polybutadiene Networks at Small Strains and Estimate of the Front Factor

S. Hvidt,[1a] O. Kramer,*[1a] W. Batsberg,[1b] and J. D. Ferry[1c]

Departments of Chemistry, University of Copenhagen, Universitetsparken 5, 2100 Copenhagen, Denmark, Risø National Laboratory, DK-4000 Roskilde, Denmark, and University of Wisconsin, Madison, Wisconsin 53706. *Received September 10, 1979*

ABSTRACT: Linear 1,2-polybutadiene with a 1,2-content of 88% is cross-linked with 10-MeV electrons in states of equibiaxial extension, pure shear, and simple extension. By use of the ideal Gaussian two-network theory, all three types of deformation give the same entanglement contribution to the equilibrium modulus after extrapolation to zero strain, $G_N = 0.70$ MPa. This agrees well with the pseudoequilibrium modulus of un-cross-linked 1,2-polybutadiene, $G_N^\circ = 0.66$ MPa. The modulus contribution of the cross-link network is $G_X \simeq 0.25$ MPa, i.e., about one-third the entanglement contribution. All moduli are given at 323 K. The two-network theory in combination with a gel-dose determination allows an estimate of the front factor of the theory of rubber elasticity to be made.

For a phantom network, the molecular theory of rubber elasticity[2,3] predicts a modulus which is proportional to the concentration of network strands, ν, the gas constant, R, and absolute temperature, T. The stress–strain relation for simple extension has the form of eq 1, where σ is the

$$\sigma = g\nu RT(\lambda - \lambda^{-2}) \quad (1)$$

engineering stress, λ is the extension ratio, and g is the front factor. The numerical value of g has been open to dispute. However, for a phantom network with tetrafunctional junctions there now seems to be general agreement that g is equal to one-half.[4]

Some studies,[5–12] all of which are based on cross-linking of long linear chains, have shown equilibrium elastic moduli which are several times higher than predicted by eq 1. This effect is thought to be due to so-called trapped entanglements. For linear polymer chains which are cross-linked to a high degree,[10–12] the magnitude of the entanglement contribution at elastic equilibrium is found to be approximately equal to the pseudoequilibrium rubber plateau modulus of the un-cross-linked polymer. However, studies based on end-linking[13–20] of short chains indicate no or only small contributions from chain entangling, when no corrections for incomplete reaction are made. The latter results are in rather good agreement with the modified theory of Flory.[4,21–23] When incomplete reaction is taken into account, the results from end-linked networks may also be interpreted in terms of substantial entanglement contributions.[24,25]

The present work was initiated in order to investigate whether the entanglement contribution, as determined from the two-network method,[7] is independent of the type of strain during cross-linking. Results from simple extension, equibiaxial extension, and pure shear are compared.

Theory

It has often[5,6,26–28] been assumed that the total concentration of elastically effective network strands is equal to the sum of a contribution from elastically effective strands terminated by chemical cross-links and a contribution from trapped entanglements. In the two-network theory[29,30] for Gaussian chains it has been shown that the strain free energy of the composite network may be expressed as the sum of two terms, the first term referring to the unstrained state and the second term referring to the state in which the second network is formed. In the two-network method,[7] trapped entanglements play the role of the first-stage network.

It was found in the previous work[7,10,31] that the Gaussian two-network theory is inadequate at larger strains in simple extension. A Mooney–Rivlin two-network description[10,31,32] gave a much better fit to the data. Also, in the previous work,[7,10,31] the two contributions were expressed in terms of network strand densities calculated on the assumption that the front factor is unity. However, the two contributions may be expressed in terms of moduli without the need of this assumption.

It is assumed in the present study that the strain free energy of the composite network may be described by the two-network theory,[29,30] as it applies to Gaussian chains. Therefore, data extrapolated to zero strain will be used throughout. The strain free energy at extension ratios λ_x, λ_y, and λ_z is

$$\Delta A_{el} = \tfrac{1}{2}G_N(\lambda_x^2 + \lambda_y^2 + \lambda_z^2 - 3) + \tfrac{1}{2}G_X(\lambda_x^2\lambda_{0x}^{-2} + \lambda_y^2\lambda_{0y}^{-2} + \lambda_z^2\lambda_{0z}^{-2} - 3) \quad (2)$$

G_N and G_X are shear moduli of the entanglement and cross-link networks, respectively; λ_{0x}, λ_{0y}, and λ_{0z} are the extension ratios during cross-linking in the strained state.

The state-of-ease extension ratios λ_{sx}, λ_{sy}, and λ_{sz} are determined by the minimum value of ΔA_{el}, subject to the condition of incompressibility ($\lambda_x\lambda_y\lambda_z = 1$). One of the features implicit in eq 2 is that the state-of-ease of the composite network is elastically isotropic,[30] and simple extension behavior relative to the state-of-ease is neo-Hookean:

$$\sigma_s = G_s(\Lambda - \Lambda^{-2}) \quad (3)$$

σ_s is the engineering stress, G_s is the modulus of the composite network in deformations from the state-of-ease, and Λ is the extension ratio in simple extension relative to the state-of-ease. G_s may be derived from eq 2. According to Flory[30]

$$G_s = G_N\left[\left(1 + \frac{G_X}{G_N}\lambda_{0x}^{-2}\right)\left(1 + \frac{G_X}{G_N}\lambda_{0y}^{-2}\right) \times \left(1 + \frac{G_X}{G_N}\lambda_{0z}^{-2}\right)\right]^{1/3} \quad (4)$$

It was also shown by Flory[30] that the extension ratios in the state-of-ease are given by

$$\lambda_{si} = [G_s/(G_N + G_X\lambda_{0i}^{-2})]^{1/2} \quad (5)$$

$$i = x, y, z$$

The extension ratios in the three directions are not inde-

0024-9297/80/2213-0933$01.00/0

Table I
Specification of Extension Ratios

	simple elongation	equibiaxial extension	pure shear
λ_x	λ	λ	λ
λ_y	$\lambda^{-1/2}$	λ	1
λ_z	$\lambda^{-1/2}$	λ^{-2}	λ^{-1}

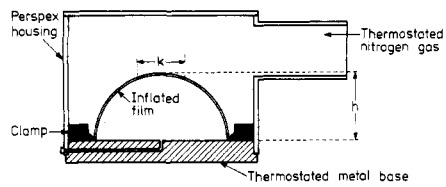

Figure 1. Irradiation cell shown with an inflated spherical bubble. Height of the bubble, h, and chord length, k, between two fiducial marks on the bubble are shown.

pendent due to incompressibility and symmetry in the various cross-linking geometries. Table I lists the specification of extension ratios used in our analysis.

From eq 2–5 and Table I it is now possible to derive the stress–strain expressions for the various cross-linking geometries.

Samples Cross-Linked in Simple Extension. Using the extension ratios given in Table I, the strain free energy becomes

$$\Delta A_{el} = \tfrac{1}{2}G_N(\lambda^2 + 2\lambda^{-1} - 3) + \tfrac{1}{2}G_X(\lambda^2\lambda_0^{-2} + 2\lambda_0\lambda^{-1} - 3) \quad (6)$$

The state-of-ease extension ratio, $\lambda_s = \lambda_{sx}$, is found as the λ value at which the derivative of ΔA_{el} with respect to λ becomes zero, and hence

$$\frac{G_X}{G_N} = \frac{\lambda_s^3\lambda_0^2 - \lambda_0^2}{\lambda_0^3 - \lambda_s^3} \quad (7)$$

The modulus of the composite network is calculated from eq 4

$$G_s = G_N\left[\left(1 + \frac{G_X}{G_N}\lambda_0^{-2}\right)\left(1 + \frac{G_X}{G_N}\lambda_0\right)^2\right]^{1/3} \quad (8)$$

From experimental values of the extension ratios during cross-linking, λ_0, and in the state-of-ease, λ_s, together with stress–strain measurements relative to the state-of-ease, the moduli G_N and G_X may now be calculated from eq 3, 7, and 8.

Samples Cross-Linked in Equibiaxial Extension. With this geometry the strain free energy becomes

$$\Delta A_{el} = \tfrac{1}{2}G_N(2\lambda^2 + \lambda^{-4} - 3) + \tfrac{1}{2}G_X(2\lambda^2\lambda_0^{-2} + \lambda_0^4\lambda^{-4} - 3) \quad (9)$$

The state-of-ease is again determined from the minimum in ΔA_{el}

$$\frac{G_X}{G_N} = \frac{\lambda_s^6\lambda_0^2 - \lambda_0^2}{\lambda_0^6 - \lambda_s^6} \quad (10)$$

The modulus of the composite network is

$$G_s = G_N\left[\left(1 + \frac{G_X}{G_N}\lambda_0^{-2}\right)^2\left(1 + \frac{G_X}{G_N}\lambda_0^4\right)\right]^{1/3} \quad (11)$$

Equibiaxial extension is achieved by inflating a polymer sheet into a bubble as shown in Figure 1. In this case we can calculate the engineering stress from the well-known hoop-stress[33] equation, giving

$$\sigma_s = (Pr/2t_s)\Lambda \quad (12)$$

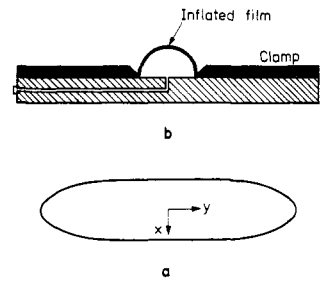

Figure 2. Pure-shear clamp. (a) Top view of the clamp hole with x and y directions indicated. (b) End view of clamp with inflated cylindrically shaped film.

where P is the pressure difference across the polymer sheet, r the radius of curvature, t_s the thickness in the state-of-ease, and Λ the extension ratio in the x and y directions relative to the state-of-ease. The stress–strain relation in equibiaxial extension is

$$\sigma_s = G_s(\Lambda - \Lambda^{-5}) \quad (13)$$

G_s may be determined from eq 12 and 13, or, alternatively, from simple extension measurements performed on strips cut from the film together with eq 3. The values of G_N and G_X are found from eq 10 and 11.

Samples Cross-Linked in Pure Shear. With this geometry, the strain free energy becomes

$$\Delta A_{el} = \tfrac{1}{2}G_N(\lambda^2 + \lambda^{-2} - 2) + \tfrac{1}{2}G_X(\lambda^2\lambda_0^{-2} + \lambda_0^2\lambda^{-2} - 2) \quad (14)$$

The stress σ in the x direction (relative to the undeformed state) is found by differentiating ΔA_{el} with respect to λ

$$\sigma = G_N(\lambda - \lambda^{-3}) + G_X(\lambda\lambda_0^{-2} - \lambda_0^2\lambda^{-3}) \quad (15)$$

We must now distinguish between two different states-of-ease. In the *constrained pure shear* state-of-ease, $\lambda_y = 1$. In the *true* state-of-ease, the sample is unclamped, and $\lambda_y \neq 1$. In the constrained pure shear state-of-ease $\sigma = 0$ and $\lambda = \lambda_s$

$$\frac{G_X}{G_N} = \frac{\lambda_s^4 - 1}{\lambda_0^2 - \lambda_s^4\lambda_0^{-2}} \quad (16)$$

Pure shear is achieved by inflating a polymer sheet into a cylindrically shaped bubble (see Figure 2). In this case the engineering stress relative to the constrained pure shear state-to-ease is given by

$$\sigma_s = Pr/t_s \quad (17)$$

where t_s is the film thickness in the constrained pure shear state-of-ease. Introducing $\sigma_s = \sigma\lambda_s$ and $\lambda = \Lambda\lambda_s$ in eq 15, we obtain

$$\sigma_s = G_N(\Lambda\lambda_s^2 - \Lambda^{-3}\lambda_s^{-2}) + G_X(\Lambda\lambda_s^2\lambda_0^{-2} - \lambda_0^2\lambda_s^{-2}\Lambda^{-3}) \quad (18)$$

The moduli G_N and G_X may now be calculated by eq 16–18.

The modulus of the composite network is found from eq 4

$$G_s = G_N\left[\left(1 + \frac{G_X}{G_N}\lambda_0^{-2}\right)\left(1 + \frac{G_X}{G_N}\lambda_0^2\right)\left(1 + \frac{G_X}{G_N}\right)\right]^{1/3} \quad (19)$$

G_N and G_X may then, alternatively, be determined, by eq 3, 16, and 19, from simple extension measurements relative to the true state-of-ease. Strips may be cut in both the x and y directions (see Figure 2).

The measured film thickness, t^*, in the true state-of-ease equals $t_s\lambda_{sz}\lambda_s$, where λ_{sz} is given by eq 5.

Determination of Radius of Curvature and Arc Length. The shapes of the inflated polymer films are approximated by those of true spheres or cylinders. This approximation has been discussed by Joye et al.[33] and was found to give correct estimates of the radius of curvature, r, within a few percent.

With this approximation, r is calculated from the diameter, $2a$, of the clamp hole and the height of the bubble, h, as illustrated in Figure 1

$$r = (a^2 + h^2)/2h \qquad (20)$$

The r values, so determined, are used to calculate the stress and to convert the measured chord length, k, into the arc length, l. The relation between k and l for an ideal sphere or cylinder is

$$l = 2r \text{ Arcsin } (k/2r) \qquad (21)$$

Experimental Section

Polymer. The 1,2-polybutadiene material used in this study was identified as polymer B in previous studies.[31,34] The composition is 88.4% vinyl, 4.7% cis, and 6.9% trans. The number- and weight-average molecular masses are 236 and 291 kg mol^{-1}, respectively, the glass-transition temperature is 255 K, the density is 885 kg m^{-3}, and the linear thermal expansion coefficient is found[35] to be 2.18×10^{-4} K^{-1} above 255 K and 0.78×10^{-4} K^{-1} below 255 K. Films with a final thickness of 0.3 mm are cast on cellophane from a 5% solution in benzene. Casting is done on a flat cast-iron table and not on mercury as used before.[7] The thickness variation on the resulting film is less than 1%. Prior to irradiation, the film is glued [with poly(cyanoacrylate)] onto the clamp of the irradiation cell and provided with ink marks. The cellophane backing is removed at least 1 h before any length measurements are made.

Radiation Source. The radiation source is a 10-MeV electron accelerator from the Haimson Research Corp. The electrons are emitted in pulses with a maximum duration of 4 μs and a maximum pulse rate of 12.5 pulses/s. A typical current in the pulse is 500 mA. Cross-linking is performed with a straight-ahead beam and a fixed position of the irradiation cell.

Dose Measurements. The dose distribution in the irradiation cell is determined by means of radiochromic film dosimeters [poly(vinylbutyral) films[36]]. The irradiation cell is used as a charge collector which is discharged through a resistor. Integration of the charge-collector voltage allows monitoring of the dose. Calibration is done with radiochromic films.

Gel Measurements. The gelation dose is determined for 1,2-polybutadiene purified by dissolution in benzene followed by precipitation in methanol. Before irradiation, the purified polymer is dried under vacuum at room temperature for 3 weeks.

Irradiation is performed with a scanning beam, and each dose is determined as the mean of three water dosimeter values. The amount of insoluble material after a given irradiation dose is determined by Soxhlet extraction in toluene. The extraction is performed under a nitrogen atmosphere for at least 72 h. Then the samples are dried under vacuum at 323 K until a constant weight is obtained. The gel content is calculated from the weight loss and the initial weight of the sample.

Irradiation Cell. The irradiation cell is shown in Figure 1. It consists of a metal base which can be thermostated with a liquid, and a cell housing made from poly(methyl methacrylate). The housing is provided with an inlet from a gas thermostat. The gas outlets are small holes through the housing just above the clamp. The thermocouple is positioned inside the housing. The thermocouple is made from very thin wires to minimize heating during irradiation. Irradiation takes place through the top window.

Temperature Control. The base of the irradiation cell is thermostated with a refrigerated circulator, using methanol as the thermostating liquid. Temperatures down to 233 K can be obtained.

The housing is thermostated with nitrogen gas. Liquid nitrogen is boiled off with an adjustable rate and heated with a two-step heater. Both heating elements are controlled by a HETO Pt-100 control unit. With this gas thermostat, the temperature in the housing of the irradiation cell may be decreased by 30 K in less than 30 s. Temperatures below 170 K are obtainable.

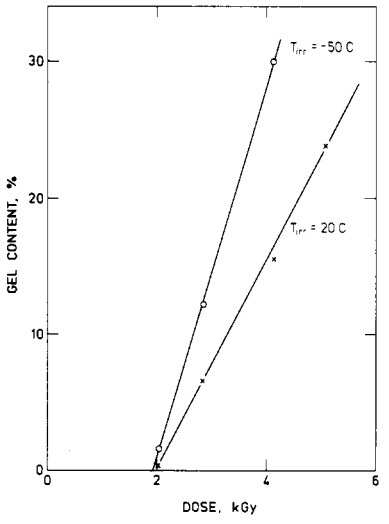

Figure 3. Plot of gel content vs. irradiation dose for two different irradiation temperatures.

Procedure. The distance between fiducial marks on the sample is measured at room temperature. The film, which is glued onto the clamp, is then positioned on the base, at 0 °C. After tightening of the screws, the temperature is lowered to −10 °C and kept constant for 10 min. The film is then slowly blown up with cold nitrogen gas through a hole in the base, and 30 s later, both thermostats are put on maximum cooling. The film becomes hard ($T < T_g$) in less than 15 s, and −40 °C is reached in less than 60 s. When the temperature has stabilized at about −40 °C, the film is irradiated with a dose of about 125 kGy (=12.5 Mrd). In the present series of experiments, all samples received approximately the same dose.

After irradiation, chord and height of the blown-up film are measured at −40 °C. The temperature is then raised to −10 °C and kept constant for 5 min in an effort to allow trapped radicals to react in the fully strained state. However, in some cases the films decreased in size when heated above the glass-transition temperature, probably owing to leakage between base and clamp.

For simple extension, a slightly modified procedure is used. Thin strips (3 cm × 0.3 cm) are stretched between pairs of springs mounted on a circular clamp. Eight samples are irradiated simultaneously.

Stress–Strain Measurements. Stress–strain measurements are made at 50 °C. In the case of simple extension, weights are suspended from the bottom clamp and the new length is measured 15 min later with a traveling microscope. In the case of equibiaxial extension and pure shear, stress–strain data are obtained by measuring sets of pressure, height, and chord length of a blown-up film; the pressure is measured with a mercury manometer. For all three types of deformation, the state-of-ease length is determined from small strains by linear extrapolation to zero force.

Simple extension is also performed on thin strips cut from samples which were cross-linked in states of equibiaxial extension and pure shear, respectively. The simple extension modulus is obtained by extrapolation to zero strain.

Results

Gel Dose. Figure 3 shows a plot of gel content vs. irradiation dose for two different irradiation temperatures. Linear extrapolation gives a dose of 2.0 kGy for incipient gel formation.

Stress–Strain. Representative stress–strain curves are shown in Figure 4. The solid curves are calculated from the Gaussian two-network theory in the case of simple extension by fitting to data of small strains. Unfortunately, the samples broke at rather small extension ratios. This is probably due to a rather high degree of cross-linking, $G_s \simeq 1.0$ MPa or an apparent network strand molecular

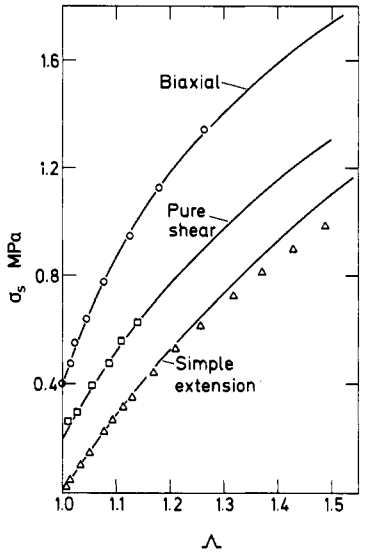

Figure 4. Stress-strain data at 323 K for samples cross-linked in different types of deformation, as indicated. After irradiation, each sample was tested in the same type of deformation that was used during the irradiation. The indicated scale is for simple extension. Other curves are shifted vertically by 0.2 and 0.4 unit. Solid lines are calculated from the Gaussian theory by fitting to data at small strains.

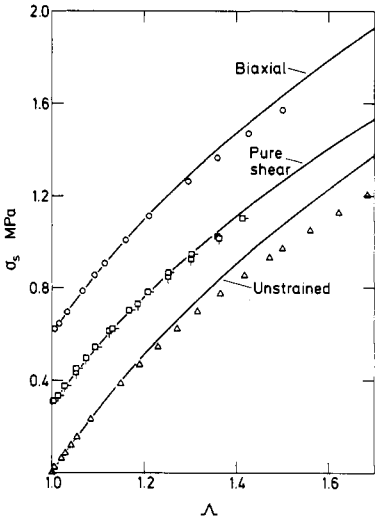

Figure 5. Simple extension stress-strain data at 323 K for samples cross-linked in different types of strain, as indicated. The scale is for unstrained. Other curves are shifted vertically by 0.3 and 0.6 unit. Solid lines are calculated from the Gaussian theory and in the case of biaxial and pure shear, by using moduli which were determined from inflation experiments. The pure-shear sample was tested in both the x direction (⊐) and y direction (⊏).

mass of about 2.5 kg mol^{-1} with a front factor of 1.

Figure 5 shows simple extension results for samples which were cross-linked in the unstrained state, in pure shear, or in equibiaxial extension. The solid lines are calculated from the Gaussian two-network theory, using moduli which for pure shear and equibiaxial extension have been determined from inflation experiments. For pure shear, results are shown for both x and y directions.

Modulus. Composite-network moduli, G_s, determined from simple extension experiments relative to the state-of-ease are shown in Figure 6. Modulus contributions from entanglements, G_N, and chemical cross-links, G_X, respectively, are calculated from the Gaussian two-network theory, using inflation measurements for pure shear and equibiaxial extension. G_X is also shown in Figure 6 while G_N is shown in Figure 7.

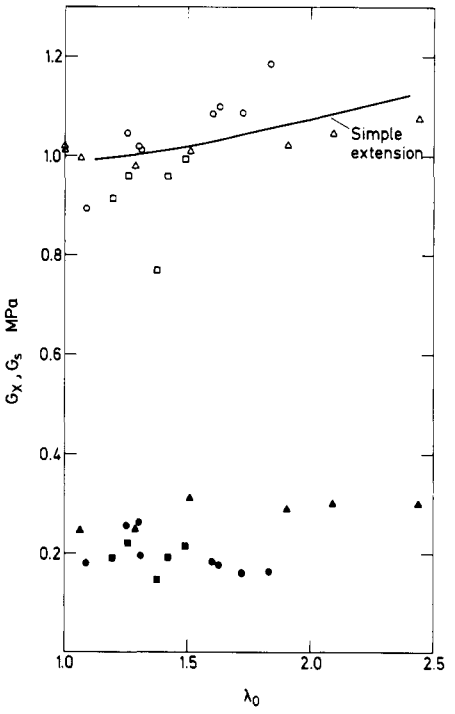

Figure 6. Composite-network modulus, G_s, and modulus contribution from chemical cross-links, G_X (filled symbols), plotted against extension ratio during cross-linking, λ_0: (○) equibiaxial; (□) pure shear; (△) simple extension. The solid curve (simple extension) is calculated from the Gaussian two-network theory with G_X = 0.26 MPa and G_N = 0.73 MPa.

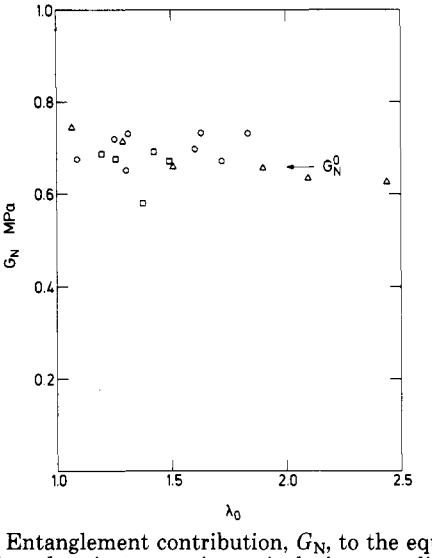

Figure 7. Entanglement contribution, G_N, to the equilibrium modulus plotted against extension ratio during cross-linking, λ_0: (○) equibiaxial; (□) pure shear; (△) simple extension. G_N^0 is the pseudoequilibrium rubber plateau modulus at 323 K of a polymer with a similar microstructure.[37]

The scatters in G_s and G_X seem to be strongly correlated. They are thought to arise primarily from dose variations. However, all the simple extension samples are irradiated simultaneously with a dose variation across the beam of less than 10%. The solid curve in Figure 6 is calculated from the two-network theory, using eq 8 with extrapolated values of G_X and G_N (from Figures 6 and 7). The curves for pure shear and equibiaxial extension are not shown. They would show increasing curvature in the order mentioned.

The entanglement contribution to the modulus, G_N, shows much less scatter, as seen from Figure 7. This is to be expected since the trapping of entanglements is

Table II
Extension Ratios and Moduli for All the Samples

type of def	sample no.	λ_0	λ_s	composite-network modulus G_s, MPa: inflation	composite-network modulus G_s, MPa: simple extension	
unstrained	32	1	1		1.02	
	38	1	1		1.02	
simple extension	31	1.068	1.016		1.00	
	37	1.290	1.063		0.98	
	33	1.512	1.125		1.01	
	36	1.904	1.179		1.02	
	34	2.093	1.216		1.04	
	35	2.440	1.262		1.08	
equibiaxial extension	18	1.091	1.020	0.87	0.89	
	12	1.255	1.074	1.00	1.04	
	21	1.304	1.098	0.97	1.02	
	16	1.312	1.076	0.98	1.01	
	20	1.604	1.163	1.04	1.08	
	19	1.630	1.164	1.08	1.10	
	22	1.722	1.192	1.03	1.08	
	17	1.833	1.222	1.16	1.19	
pure shear	11	1.198	1.041		0.90[a]	0.93[b]
	15	1.259	1.060		0.96[a]	0.96[b]
	25	1.378	1.070		0.78[a]	0.76[b]
	14	1.422	1.083		0.95[a]	0.97[b]
	13	1.492	1.106		1.01[a]	0.98[b]
	27[c]	2.372	1.347		0.96[a]	
	26[c]	3.813	1.377		0.93[a]	0.92[b]

[a] Simple extension in x direction (see Figure 2). [b] Simple extension in y direction (see Figure 2). [c] Not pure shear, $\lambda_y > 1$ (see Figure 2).

nearly complete at such high degrees of cross-linking. Incorrectly determined λ_s and λ_0 extension ratios may also cause scatter in G_N and G_X, individually, whereas the sum of G_N and G_X should be only slightly affected.

The pseudoequilibrium modulus, $G_N°$, of un-cross-linked 1,2-polybutadiene with a similar microstructure[37] is also shown in Figure 7. The value has been corrected to 323 K.

Extension ratios and moduli for all samples are summarized in Table II. For samples cross-linked in pure shear, simple extension moduli are reported for both x and y directions.

Discussion

The new equipment for irradiation with 10-MeV electrons instead of γ-irradiation has resulted in more experimental freedom with respect to sample geometry, type of deformation, irradiation time, and relaxation prior to cross-linking. However, the dose repeatability of the linear accelerator is not as good as for the ^{60}Co sources used previously.[7,10,38] The scatter in Figure 6 indicates that we have not been able to keep the dose constant. The dose variation is estimated to be about 25%. Fortunately, small variations in dose have very little effect on the entanglement contribution to the equilibrium modulus, as can be seen in Figure 7.

Small Strains. All three types of strain give nearly the same entanglement contribution, G_N, to the equilibrium modulus. Extrapolation to zero strain for all samples combined gives $G_N = 0.70$ MPa. This compares very well with the pseudoequilibrium modulus of the un-cross-linked polymer, $G_N° = 0.66$ MPa.[37] A comparison to the stress relaxation modulus of the un-cross-linked polymer may also be made. The stress relaxation at −10 °C prior to cross-linking corresponds to a little less than 1 s at 0 °C. In Figure 2 of the paper by Noordermeer and Ferry,[34] $t = 1$ s corresponds to the first experimental point, $G(t) \simeq 0.7$ MPa at 0 °C. Multiplication by the ratio 323/273 gives $G(t) \simeq 0.8$ MPa at 50 °C. This value also compares very well to $G_N = 0.70$ MPa.

For all samples combined, the scatter in the G_N values of Figure 7 is less than ±10%. More scatter is observed for the G_X values in Figure 6, indicating large dose variations. It seems that the simple extension samples in particular have received a high dose. Linear extrapolation of the simple extension results to zero strain gives $G_X = 0.26$ MPa and $G_N = 0.73$ MPa. The sum is 0.99 MPa, which compares very well with the experimentally found composite-network modulus for samples cross-linked in the unstrained state, $G_s = 1.02$ MPa (see Figure 6).

Large Strains. The two-network theory may be tested on individual samples by performing stress–strain measurements relative to the state-of-ease or by comparing moduli for different samples as a function of extension ratio during cross-linking.

For simple extension relative to the state-of-ease, the simple Gaussian two-network theory clearly does not predict the observed behavior. This is true for samples which are cross-linked in states of simple extension, as has been reported previously by Ferry and co-workers.[7,10,31,32] However, it is also true for samples cross-linked in states of pure shear or equibiaxial extension, as shown in Figure 5.

When different simple extension samples are compared, deviations from expected behavior are also found. In Figure 6 the observed G_s values for simple extension fall progressively short of the predicted values, and the calculated G_N values in Figure 7 decrease with increasing λ_0. Several aspects of non-Gaussian behavior will be reported in a forthcoming publication.

For samples cross-linked in states of pure shear or equibiaxial extension, dose variations are too large to allow a comparison between observed and predicted moduli as a function of the extension ratio during cross-linking. Stress–strain behavior in pure shear and equibiaxial extension, respectively (see Figure 4), seems to follow the simple Gaussian two-network theory quite well. However, the precision of the inflation measurements is not as good as for the simple extension measurements, and the inflated samples have a tendency to break at rather low extensions. Therefore, the present experiments cannot exclude the possibility of small deviations from the theory.

Front Factor. The two-network method permits, at least in theory, a complete separation of the modulus contributions from chemical cross-links and entanglements, respectively. The two-network method, in combination with an independent estimate of the number of cross-linked units from gel-point measurements, therefore, allows a determination of the front factor g in eq 1 with the direct entanglement contribution removed. However, several experimental conditions must be fulfilled as discussed in the Appendix.

The functionality of the chemical cross-links is a serious problem in the present work. This is especially true for polybutadienes of high vinyl content since the vinyl units may participate in a chain reaction.[9] The mean functionality of the chemical cross-links has been found to be equal to 4.4[11] for a polybutadiene with a vinyl content of 8%. For a polybutadiene with a vinyl content of 88%, the mean functionality should be expected to be somewhat higher. Values of about 4.8[9] for irradiation in air at room temperature have been reported. In the Appendix, the value of the front factor has been calculated for functionalities of 4 and 6.

The lower value, $f = 4$, gives $g = 0.5 \pm 0.1$; the upper value, $f = 6$, gives $g = 1.1 \pm 0.2$. The theoretical values

for a phantom network are 0.5 and 0.67,[4] respectively. The theoretical value for affine deformation is 1.0.[4]

It can be seen that the two-network method, after removal of a very large entanglement modulus contribution, gives g values which are in reasonable agreement with the values predicted from phantom-network theory and affine theory. However, the above range of values, $0.5 < g < 1.1$, is too large to allow a distinction between the two types of behavior. Provided a better polymer with a more clearly defined functionality could be found, it should be possible to determine the g value with a precision of 10–20%. The ideal polymer for this purpose should have an extremely high molecular weight, no chain scission, and a uniform functionality of the cross-links. Experiments with two new polymers are planned.

If the composite-network modulus, $G_s \simeq 1.0$ MPa, instead were to be ascribed to chemical cross-links, alone, much higher g values would result. Assuming tetrafunctional cross-links, g would come out to be 2.0; assuming hexafunctional cross-links, g would come out to be 4.2. Both of these values are much higher than the prediction of any theory.

Conclusion

Assuming applicability, at least for small strains, of the Gaussian two-network theory in the form of eq 2, the two-network method gives the following results for the case of negligible stress relaxation prior to cross-linking:

1. The entanglement contribution, G_N, to the equilibrium modulus is equal to the pseudoequilibrium entanglement modulus of the un-cross-linked polymer, G_N°, independent of type of deformation.

2. The direct contribution to the modulus from chemical cross-links, G_X, is much smaller than the contribution from entanglements; $G_X \simeq {}^1/_3 G_N$ for the present samples which are highly cross-linked.

These results are in excellent agreement with the results of Graessley and co-workers,[11,12] and it should be emphasized that above results are obtained without the need to determine or make any assumptions about the front factor, the functionality of the chemical cross-links, the gel point, or the degree of cross-linking.

Acknowledgment. We gratefully acknowledge the assistance of the Accelerator Department, Risø National Laboratory, where all irradiations were performed. Special thanks to A. Miller, D. Heldrup, and C. Nawrocki. The work was supported, in part, by NATO Research Grant No. 935.

Appendix

Estimate of the Front Factor. The front factor can be determined from the two-network method, provided the following experimental conditions are fulfilled: (a) negligible relaxation prior to cross-linking in the strained state; (b) negligible chain scission; (c) random cross-linking and proportionality of dose and cross-linking; (d) accurate values of molecular weight ($\bar{M}_w$ and $\bar{M}_n$), gel dose, and cross-linking dose; (e) cross-links of known functionality.

If considerable relaxation were to occur, the modulus of the network formed in the strained state would include a contribution from relaxed entanglements.[39] The relaxation prior to cross-linking is negligible in the present experiments.

Negligible chain scission may not be an absolute requirement, but to take chain scission into account would meet with both experimental and theoretical difficulties. Chain scission is found to be very small for polybutadienes of high 1,2-content, less than about one scission per 100 cross-linked units.[9]

Proportionality of dose and the number of cross-linked units seems to be a reasonable assumption since the fraction of cross-linked units is very small, of the order of 1%. It has been suggested by Flory, as referred to in a paper by Falender et al.,[40] that the gel point may be delayed due to nonrandom cross-linking which is caused by the spur effect of high-energy irradiation. Such a delay in the gel point would lead to a fictitiously low estimate of the degree of cross-linking and thus result in too large a value of the front factor.[40] Heilmann[41] considers clusters of a relatively small number of closely spaced cross-links. If a cluster of cross-links should give rise to more than one cross-link on one of the chains, the effect on the gel point may be compared to that of multifunctional cross-links. Heilmann[41] predicts that the overall effect, if anything, should be an enhancement rather than a delay in the gel formation.

Molecular weights and gel dose are known with a reasonable accuracy, better than 10% for each. The cross-linking dose for the individual samples is not known with a satisfactory accuracy in the present experiments, about ±20%. However, it should be possible to improve the dose determination to better than 10%.

The functionality of the chemical cross-links is a serious problem. The functionality, f, must be known in order to estimate the number of cross-linked units per chain, and for comparison with theory which predicts $g = (f - 2)/f$ for a phantom network.[4] It may be shown from eq 5 in a paper by Pearson and Graessley[28] that at the gel point, the number of cross-linked units per chain (uniform molecular weight) is equal to $2/(f - 2)$, i.e., 1, ${}^1/_2$, and ${}^1/_3$ for tetra-, hexa-, and octafunctional junctions, respectively.

The gel dose is 2.0 kGy, and the mean dose for all irradiations is estimated to be 125 kGy. For tetrafunctional cross-links, this gives 63 cross-linked units per weight average chain. Sixty-three cross-linked units correspond to sixty-four strands per weight average chain or a mean strand molecular mass of $291/64 = 4.55$ kg mol^{-1}. Discounting the two free chain ends,[42] we can express the modulus as

$$G_X = g\frac{\rho}{M_c}RT\left(1 - \frac{2M_c}{\bar{M}_n}\right) \qquad (22)$$

where G_X is the modulus contribution from chemical cross-links, ρ is density, M_c is mean strand molecular weight, and $\bar{M}_n$ is number-average molecular weight. The G_X values are taken from Figure 6. Linear extrapolation to zero strain gives $G_X = 0.26$ MPa for simple extension and $G_X = 0.23$ MPa for pure shear and biaxial extension combined. Equation 22 gives $g = 0.52$ for simple extension and $g = 0.46$ for pure shear and biaxial extension.

Assuming hexafunctional junctions, the number of cross-linked units at the gel point is reduced by a factor of 0.5. The g values would therefore be 1.1 for simple extension and 1.0 for pure shear and equibiaxial extension.

References and Notes

(1) (a) University of Copenhagen. (b) (b) Risø National Laboratory. (c) University of Wisconsin.
(2) Treloar, L. R. G. "The Physics of Rubber Elasticity", 3rd ed.; Clarendon Press: Oxford, 1975.
(3) Smith, T. L. *Treatise Mater. Sci. Technol.* **1977**, *10*, 369.
(4) Flory, P. J. *Proc. R. Soc. London, Ser. A* **1976**, *351*, 351–78.
(5) Moore, C. G.; Watson, W. F. *J. Polym. Sci.* **1956**, *19*, 237–54.
(6) Meissner, B. *J. Polym. Sci., Part C* **1967**, *16*, 781–92.
(7) Kramer, O.; Carpenter, R. L.; Ty, V.; Ferry, J. D. *Macromolecules* **1974**, *7*, 79–84.
(8) Langley, N. R.; Polmanteer, K. E. *J. Polym. Sci., Polym. Phys. Ed.* **1974**, *12*, 1023–34.
(9) Pearson, D. S.; Skutnik, B. J.; Böhm, G. G. A. *J. Polym. Sci., Polym. Phys. Ed.* **1974**, *12*, 925–39.

(10) Carpenter, R. L.; Kramer, O.; Ferry, J. D. *Macromolecules* **1977**, *10*, 117–9.
(11) Dossin, L. M.; Graessley, W. W. *Macromolecules* **1979**, *12*, 123–30.
(12) Dossin, L. M.; Pearson, D. S.; Graessley, W. W. *Polym. Prepr., Am. Chem. Soc., Div. Polym. Chem.* **1979**, *20*, 224–7.
(13) Kraus, G.; Moczygemba, G. A. *J. Polym. Sci., Part A* **1964**, *2*, 277–88.
(14) Rempp, P.; Herz, J.; Hild, G.; Picot, C. *Pure Appl. Chem.* **1975**, *43*, 77–96 and several references cited therein.
(15) Froehlich, D.; Crawford, D.; Rozek, T.; Prins, W. *Macromolecules* **1972**, *5*, 100–2.
(16) Walsh, D. J.; Allen, G.; Ballard, G. *Polymer* **1974**, *15*, 366–72.
(17) Allen, G.; Holmes, P. A.; Walsh, D. J. *Faraday Discuss. Chem. Soc.* **1974**, *No. 57*, 19–26.
(18) Mark, J. E.; Sullivan, J. L. *J. Chem. Phys.* **1977**, *66*, 1006–11.
(19) Mark, J. E.; Rahalkar, R. R.; Sullivan, J. L. *J. Chem. Phys.* **1979**, *70*, 1794–7.
(20) Llorente, M. A.; Mark, J. E. *J. Chem. Phys.* **1979**, *71*, 682–9.
(21) Ronca, G.; Allegra, G. *J. Chem. Phys.* **1975**, *63*, 4990–7.
(22) Flory, P. J. *J. Chem. Phys.* **1977**, *66*, 5720–9.
(23) Flory, P. J. *Polymer* **1979**, *20*, 1317–20.
(24) Valles, E. M.; Macosko, C. W. In "Chemistry and Properties of Crosslinked Polymers"; Labana, S. S., Ed.; Academic Press: New York, 1977; pp 401–10.
(25) Gottlieb, M.; Macosko, C. W., submitted for publication in *J. Chem. Phys.*
(26) Bueche, A. M. *J. Polym. Sci.* **1956**, *19*, 297–306.
(27) Langley, N. R. *Macromolecules* **1968**, *1*, 348–52.
(28) Pearson, D. S.; Graessley, W. W. *Macromolecules* **1978**, *11*, 528–33.
(29) Berry, J. P.; Scanlan, J.; Watson, W. F. *Trans. Faraday Soc.* **1956**, *52*, 1137–51.
(30) Flory, P. J. *Trans. Faraday Soc.* **1960**, *56*, 722–43.
(31) Carpenter, R. L.; Kramer, O.; Ferry, J. D. *J. Appl. Polym. Sci.* **1978**, *22*, 335–42.
(32) Kramer, O.; Ferry, J. D. *Macromolecules* **1975**, *8*, 87–9.
(33) Joye, D. D.; Poehlein, G. W.; Denson, C. D. *Trans. Soc. Rheol.* **1972**, *16*, 421–45.
(34) Noordermeer, J. W. M.; Ferry, J. D. *J. Polym. Sci., Polym. Phys. Ed.* **1976**, *14*, 509–20.
(35) Hvidt, S. Cand. Scient. Thesis, The University of Copenhagen, 1979.
(36) McLaughlin, W. L.; Miller, A.; Fidan, S.; Pejtersen, K.; Pedersen, W. B. *Radiat. Phys. Chem.* **1977**, *10*, 119–27.
(37) Ferry, J. D. "Viscoelastic Properties of Polymers", 2nd ed.; Wiley: New York, 1970; p 406.
(38) Kramer, O.; Ferry, J. D. *J. Polym. Sci., Polym. Phys. Ed.* **1977**, *15*, 761–3.
(39) Kan, H.-C.; Ferry, J. D. *Macromolecules* **1979**, *12*, 494–8.
(40) Falender, J. R.; Yeh, G. S. Y.; Mark, J. E. *J. Chem. Phys.* **1979**, *70*, 5324–5.
(41) Heilmann, O. J., submitted for publication in *J. Chem. Phys.*
(42) Flory, P. J. *Chem. Rev.* **1944**, *35*, 51–75.

Measurement of the Cluster Size Distributions for High Functionality Antigens Cross-Linked by Antibody

Gustav K. von Schulthess* and George B. Benedek

Department of Physics and Center for Materials Science and Engineering, and the Harvard M.I.T. Division of Health Sciences and Technology, Massachusetts Institute of Technology, Cambridge, Massachusetts 02139

Ralph W. De Blois

General Electric Corporate Research and Development Laboratory, Schenectady, New York.
Received October 16, 1979

ABSTRACT: We have measured, in situ, the evolution of the cluster size distribution of a condensing system of high functionality antigens cross-linked by antibody, using a resistive pulse analizer. The distributions were determined over the full range of values ($0 \leq b < 1$) of the bonding parameter (b) $b = (1 - 1/\bar{n})$ where $\bar{n}$ is the mean number of units in the clusters. The normalized cluster size distributions (X_n/X) are well described by the form $(X_n/X) = (1 - b)e^{-nb}(nb)^{n-1}/n!$. The critical exponents τ, α, and γ_g describing the asymptotic forms of this distribution and its second moment near the condensation point ($b = 1$) can be obtained. We find $\tau = 1.4 \pm 0.15$, $\gamma_g = 2$, and provisionally $\sigma = {}^1/_2$. The experimental distributions are compared with three different classes of theoretical predictions: the solutions of the generalized Smoluchowski kinetic equations, the equilibrium statistical distributions, and the theories of three-dimensional percolation.

The cluster size distribution of interacting particles plays a central role in the characterization of condensing systems. Such cluster size distributions occur in the study of: organic polymer reactions,[1-4] antibody–antigen agglutination reactions,[5-7] percolation processes,[8-10] gas–liquid and magnetic order–disorder phase transitions,[11-13] and colloidal[14] and aerosol[15] suspensions. The theories of the cluster size distribution usually assume thermodynamic equilibrium among the clusters for each value for the extent of the reaction.[2] Recently, modern theories of critical phenomena have drawn attention to the use of static scaling laws and critical exponents to describe the divergence of the moments of the equilibrium cluster size distributions near the critical condensation point.[16-18] On the other hand, following von Smoluchowski,[19] a number of authors[15,20-22] have focused on the kinetics of such reactions and have computed the temporal evolution of the cluster size distributions, using various mathematical forms for the interparticle reaction rates.

We report measurements of the distribution of cluster sizes, using as the interacting particles polystyrene latex spheres (diameter 0.235 μm) upon whose surface the antigen human serum albumin (hSA) has been covalently bonded. These antigen coated carrier particles (units) are cross-linked by complementary bivalent antibody molecules—goat anti-hSA introduced into the solution. The cluster size distribution was measured by using the Nanopar resistive pulse particle size analyzer devised and developed by De Blois and Bean.[23,24] This analyzer permits the measurement of the number of units in the individual clusters within our reaction mixture without disturbing the reaction kinetics.

Our reacting particles and the measurement method taken together provide a unique system for the quantitative investigation of the cluster size distribution. The use of antigen-coated carrier particles rather than polyfunctional organic molecules (units) has the effect of increasing the size of the units from ~100 Å to ~2000 Å and in-

0024-9297/80/2213-0939$01.00/0